Int. J. Appl. Math. Comput. Sci., 2025, Vol. 35, No. 3, 391–402
DOI: 10.61822/amcs-2025-0027

MATHEMATICAL ASPECTS OF CALIBRATION BY DIFFEOMORPHISMS

ROBERTO OROZCO [a,*], JOANNA RATAJCZAK [a]

[a]Department of Cybernetics and Robotics
Wrocław University of Science and Technology
Wyb. S. Wyspiańskiego 27, 50-370 Wrocław, Poland
e-mail: roberto.orozco@pwr.edu.pl

In this paper, we present a novel approach to calibrating robotic manipulators—calibration by diffeomorphisms. The method is carried out in detail, placing special emphasis on the mathematical basis of the algorithm. The main idea is based on the synergy of the theory of singular mappings and the large dense diffeomorphic metric mapping framework, a method previously unused in robotic applications, together with reproducing kernel Hilbert spaces. The proposed solution allows the determination of appropriate diffeomorphisms, which, as it were, adjust the arbitrarily chosen kinematics to match a real one, thus taking into account inaccuracies arising from inaccurately determined parameters or a previously unmodelled phenomenon, for example, due to high complexity or nonlinearities. The effectiveness of the calibration by diffeomorphisms is illustrated using a numerical experiment for a manipulator with two degrees of freedom.

Keywords: kinematics, robot kinematics calibration, diffeomorphisms, calibration by diffeomorphisms.

1. Introduction

One of the most significant features of robot manipulators is their ability to perform repeatable tasks with exceptional precision and accuracy. This capability heavily relies on the mathematical model of the robot's kinematics, a critical component of the software controller. Ensuring the correctness of this model is paramount for optimal robot performance. Typically, these models are developed during the robot's design stage using methods such as the Denavit–Hartenberg or product of exponentials algorithms. These methods create a mapping from the Cartesian product of joint space and parameter space to the task space, relying on assumptions of ideally rigid joints and links, perfectly aligned joint axes, as well as fixed dimensions and relative positions of the links, collectively defining the robot's geometry.

However, these assumptions may not hold in the final manufactured product, leading to deviations from the desired accuracy. In such cases, the mathematical model must be adjusted to maintain the required precision and accuracy.

In robotics literature, this adjustment process is known as the robot kinematics calibration problem. It can be described as follows: based on measurements of the positions of the robot joints and the corresponding end-effector poses, the nominal kinematics model is reformulated to minimize discrepancies between the predicted and actual end-effector poses according to predefined criteria.

Methodologically and algorithmically, this problem is often approached through parametric system identification. The aim is to find a set of parameter values for the nominal kinematics that better describe the observed data. Common techniques used for this purpose include the least squares or Gauss–Newton methods. These approaches allow for the refinement of the kinematics model to more accurately reflect the actual behaviour of the robot, thereby improving the level of precision and accuracy.

The primary drawback of this approach is that the solution is searched within a parametrized family of kinematics model that imposes constraints on the possible geometries. In other words, the problem can be accurately solved only if the actual kinematics fall within the scope of the considered family of kinematics, as defined by certain parameters. Unfortunately, this is not always the case. For instance, links or joints might be made from materials that are not perfectly rigid (e.g., 3D-printed components or

*Corresponding author

plastic links), or there could be joint transmission errors.

When considering the general problem of calibration (not strictly limited to manipulator kinematics), there may be unknown phenomena, potentially nonlinear, that affect the nominal model. Such errors are difficult to model or incorporate into nominal kinematics due to their complex and nonlinear behaviour. As a result, it is logical to explore a non-parametric approach.

To the best of the authors' knowledge, apart from the use of neural networks (Zhao *et al.*, 2019; Nguyen *et al.*, 2015; Gadringer *et al.*, 2020; Zhong *et al.*, 1996), non-parametric approaches have received limited attention within the robotics community. This represents a significant research gap that we aim to investigate. Motivating examples for developing general non-parametric methods include, e.g., accurate modelling of automatic telescopes (Pál *et al.*, 2015), drilling machines (Scraggs *et al.*, 2021) or mesh bed levelling procedures in the 3D printers.

For completeness, we shall mention that calibrating the kinematic or dynamic model of a robot is not the only approach to addressing uncertainties in these systems. While calibration aims to refine the model parameters to improve accuracy, an alternative strategy is to design control algorithms that are inherently robust to model uncertainties. Such control methods adapt to variations in the system without requiring precise knowledge of the exact kinematic and dynamic parameters. An example of this approach has been presented by Bonilla *et al.* (2018), with the proposed control scheme successfully handling model uncertainties without the need for explicit calibration.

The entry point of our research is the calibration by diffeomorphisms introduced by Tchoń (1992). To gently introduce the idea behind let us consider the following example. Usually, the kinematics model is mathematically expressed as a smooth mapping $k\colon X \to Y$, living in the space of smooth mappings, i.e., $k \in \mathrm{C}^\infty(X, Y)$, that takes configurations $x \in X$ as arguments and the end-effector pose $y \in Y$ (position, orientation or both) as values. With compact X and Y being smooth manifolds. Having a nominal model of kinematics, the workspace is defined as a subspace of the task space, consisting of all the end-effector's reachable poses. Using a double pendulum as a toy example of nominal kinematics, the workspace is depicted as an annulus (Fig. 1). Introducing discrepancies to the model affects this annulus; for instance, increasing the length of the links makes the annulus larger. When the discrepancies are nonlinear, the annulus will be affected non–linearly. For example, bending under gravitational force stretches the annulus vertically. Usually, the discrepancies appearing in the robotic systems are small and does not 'disrupt' the workspace. Despite these deformations, the workspace remains topologically 'similar' to the

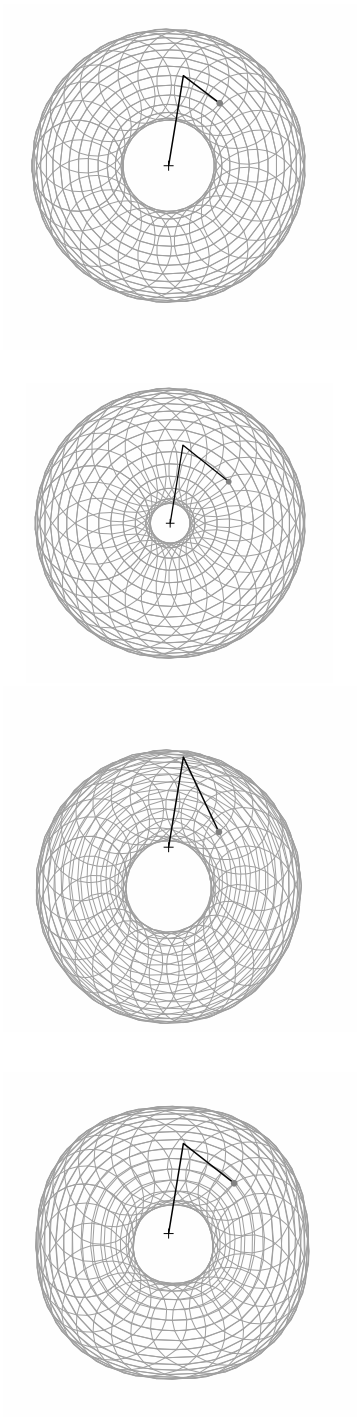

Fig. 1. Double pendulum's workspace under different discrepancies that persist the kinematics diffeomorphically equivalent to each other (top to bottom): no discrepancies, discrepancies in length parameters, gravitational bending, large non-linear diffeomorphism. The $'+'$ and $'\cdot'$ signs denotes the origin of the taskspace's coordinate frame and position of the end-effector (corresponding to the same configuration for each panel), respectively. The discrepancies are "big" for the visualisational purposes.

annulus. The mentioned observation drove Tchoń's to the conclusion that the actual kinematics may be viewed as nominal kinematics deformed by stretching, squeezing or translation. Mathematically speaking, both the actual kinematics and the nominal one are diffeomorphically equivalent to each other, i.e., it means that there exist smooth transformations with smooth inverse that transform the nominal kinematics to the actual one and backwards.

To integrate this observation into the calibration problem, used the theory of stable mapping singularities to define the problem mathematically. In this framework, calibration involves finding a pair of diffeomorphisms such that, when composed with the nominal kinematics, they yield the actual kinematics. Tchoń (1992) presents an analytical method for computing these transformations under the assumptions of structural stability and affine diffeomorphisms. However, the mathematical complexity of this approach makes it impractical for real-world applications.

In contrast, our approach relaxes these assumptions and embed the problem within a computational framework. We define calibration through the concept of A-equivalence between mappings $k' \in \mathrm{C}^\infty(X,Y)$ and $k \in \mathrm{C}^\infty(X,Y)$. Specifically, k' is A-equivalent to k if there exist diffeomorphisms $\varphi \in \mathrm{Diff}\,(X)$ and $\psi \in \mathrm{Diff}\,(Y)$ such that $k' = \psi \circ k \circ \varphi^{-1}$, $\mathrm{Diff}\,(X)$ and $\mathrm{Diff}\,(Y)$ being a group of diffeomorphisms of X and Y, respectively. Assuming k and k' are A-equivalent, we aim to design a ϑ-parametrized curve k_ϑ such that $k_\vartheta = \psi_\vartheta \circ k \circ \varphi_\vartheta^{-1}$, with endpoints $k_{\vartheta=0} = k$ and $k_{\vartheta=1} = k'$.

Importantly, the diffeomorphism ψ, composed with k from the left, addresses the discrepancies that cannot be calibrated through the diffeomorphism φ alone due to the singularities of k or the physical constraints of the robot. This differs from the simpler case (non-singular kinematics), where only one diffeomorphism is sufficient.

Framing the calibration problem this way allows us to adjust nominal kinematics to match the actual kinematics without explicitly modelling individual phenomena. Instead, discrepancies are inferred from the differences between the nominal and actual kinematics. This contrasts with traditional approaches, which rely on explicit models of discrepancies and require parameter estimation. In particular, the presented method is more flexible and offers a solution to calibration problem for cases when modelling of the discrepancies is hard.

The primary contribution of this paper is the introduction of a numerical method for calibration using diffeomorphisms. Secondly, the paper meticulously introduces the mathematical fundamentals underlying the new methodology for calibration by diffeomorphisms. To demonstrate the effectiveness of this approach, we evaluate the method on the kinematics of a simple two degree-of-freedom (DoF) double pendulum. The use of a two DoF robot kinematics model is intentional, as it avoids obscuring the properties of the algorithm with the complexity of a more intricate kinematics model.

The composition of the paper is as follows. Section 2 introduces the results of the formulation of large dense diffeomorphic metric mapping (LDDMM) framework (Beg *et al.*, 2005). The formulation of the calibration by diffeomorphisms in this framework is described in Section 3. Sections 4 and 5 evaluate the mathematical findings by simulation experiments, discuss the results and formulate future works. Finally, the summary in Section 6 concludes the paper.

2. Image registration

To make the idea of calibration by diffeomorphisms more practical and applicable we decided to embed it in the framework developed in computational anatomy, namely the large diffeomorphic metric mapping. The mentioned methodology relies on the concept of deforming the image such that it will resemble another one—topologically and differentially equivalent. This formulation was developed to solve two problems: an image registration problem and to construct a mathematical framework for comparison of the imagery and statistical purposes. In our study, we constrain ourselves to the scope of the registration problem, that in fact, is quite similar to the problem of calibration or identification in the field of control engineering and robotics. In this setup, the diffeomorphisms are computed as a flow of the vector field (the solution of an ordinary differential equation (ODE) corresponding to the vector field). In particular, it perfectly suits the calibration of diffeomorphisms. Mathematically, the problem may be formulated as follows.

2.1. Mathematical formulation. In the framework introduced by Bruveris and Holm (2015), the transformations are modelled as the elements of a Lie group G. They act on elements of the space of objects modelled as a vector space V, by a left action $(g, I) \to g \cdot I \in V$, $g \in G$, $I \in V$. The transformations are computed as a flow of a non-autonomous ordinary differential equation, and thus we shall specify it. To do that, we need the notion of a Lie algebra of a Lie group. Simply, the Lie algebra is a tangent space in the identity element, namely, $\mathfrak{g} = T_eG$. Then the non-autonomous ODE is defined as follows $\frac{\partial g_\vartheta}{\partial \vartheta} = u_\vartheta \cdot g_\vartheta$, where u_ϑ is a curve dependent on ϑ in $\mathfrak{g}$, and g_ϑ a curve in a Lie group G, i.e., the flow of u_ϑ. The right-hand side of the above equation may be interpreted as an infinitesimal action of the Lie algebra on the Lie group. The last piece of a modelling detail is to endow the Lie algebra $\mathfrak{g}$ and the

space of the object V with the inner products $\langle\cdot,\cdot\rangle_{\mathfrak{g}}$ and $\langle\cdot,\cdot\rangle_V$.

Having defined all the crucial pieces of notation, the abstract formulation of the registration problem is as follows. For a given $I_1, I_2 \in V$ find a curve $u_\vartheta \in \mathfrak{g}$ that optimizes cost function

$$\min_u \frac{1}{2}\int_0^1 \|u_\vartheta\|_{\mathfrak{g}}^2 \,\mathrm{d}\vartheta + \frac{1}{2\sigma^2}\|g_1 \cdot I_1 - I_2\|_V^2, \qquad (1)$$

subject to

$$\frac{\partial g_\vartheta}{\partial \vartheta} = u_\vartheta \cdot g_\vartheta, \quad g_0 = e, \qquad (2)$$

where e is a neutral element.

The standard approach to tackle the above optimization problem is to use variational calculus to compute the optimal condition. The careful derivation made by Bruveris and Holm (2015) yields that the minimizer is given by

$$u_\vartheta^\flat = -g_\vartheta \cdot I_1 \diamond g_\vartheta g_1^{-1} \cdot \pi, \qquad (3)$$

with $\pi = \frac{1}{\sigma^2}(g_1 \cdot I_1 - I_2)^\flat \in V^*$, where $\flat\colon TV \to T^*V$ is an isomorphism between tangent and cotangent bundle induced by the metric, and $\diamond\colon T^*V \to \mathfrak{g}^*$ being so-called momentum map that assigns for each element (I,π) of the phase space an element $I \diamond \pi$ in the dual g^* of the Lie algebra. A detailed explanation of the introduced notion, along with examples, can be found in the work of Holm *et al*. (2009).

As has been observed (Bruveris and Holm, 2015), the solution u_ϑ to the problem (1) is expressed as a momentum map, and due to conservation of the momentum, u_ϑ satisfies the Euler–Poincare equations. This allows us to reduce the problem by considering the evolution equation in the phase space T^*V. So, the registration problem may be reformulated as follows. Given $I_0, I_2 \in V$ find $P_0 \in V^*$ that minimizes

$$E(P_0) = \frac{1}{2}\|I_0 \diamond P_0\|_{\mathfrak{g}}^2 + \frac{1}{2\sigma^2}\|I_1 - I_2\|_V^2, \qquad (4)$$

where I_1 is defined as the solution of the system of equations

$$\begin{cases} \frac{\partial I_\vartheta}{\partial \vartheta} = \zeta_{u_\vartheta}(I_\vartheta), \\ \frac{\partial P_\vartheta}{\partial \vartheta} = -T^*_{I_\vartheta}\zeta_{u_\vartheta} P_\vartheta, \\ u_\vartheta^\flat \vartheta = I_\vartheta \diamond P_\vartheta, \end{cases} \qquad (5)$$

with $\zeta_{u_\vartheta}\colon V \to TV$, being a fundamental vector fields associated with the G-action.

The system of ordinary differential equations above is the entry point for settling the calibration by diffeomorphism in the computational framework.

3. Main result

In this section, we derive the equation governing calibration by diffeomorphisms. We begin by setting up basic notions to align with the abstract formulation introduced by Bruveris and Holm (2015), as discussed and recalled in the previous section. This foundation is crucial for deriving the relevant differential equations. Following this approach, we introduce the transformation group and the space in which these transformations act. Next, we define the problem using the abstract formulation and, finally, we derive the necessary equations.

3.1. Basic notions. We begin by detailing the space of objects V. These objects represent the kinematics model of a robot, so the space V should encompass all possible kinematics models. To formalize this, we introduce the notion of the kinematics model, which will be used throughout the following sections.

Generally, the mathematical model of robot kinematics is described as a mapping between the configuration space X (where the joint positions reside) and the task space Y (where the end-effector's position and orientation reside), concisely denoted as $k : X \to Y$. Typically, for n DoF manipulator with r revolute joints, X is $R^{n-r} \times T^r$, where T^r denotes the r-dimensional torus, while Y is a smooth manifold and a subgroup of the $SE(3)$ Lie group. In special cases, the configuration space and task space can be identified with the Euclidean spaces R^n and R^m, respectively. This representation specifies previously introduced notion of kinematics to a particular case, namely,

$$k\colon R^n \to R^m, \qquad (6)$$

known as kinematics in coordinates. We will focus on this particular representation for two reasons. Firstly, it describes the kinematics of several classes of robots. Starting with such kinematics representation allows us to study and develop the algorithm without the complexities that could obscure the subtleties, details and properties of the method. Secondly, to set the calibration problem within the formalism discussed in the previous section, we assume that the space of objects V is a vector space. Representing the kinematics in this form satisfies this assumption.

As a careful reader may observe, we work with kinematics in local coordinates, meaning that the solution is local. However, the method can be made global through the careful definition of vector fields on appropriate manifolds. Therefore, the generalisation of the method to more complex kinematics appears possible and is under consideration, but some challenges arise that we aim to address in the future, such as the global definition of vector fields and the curse of dimensionality. Nevertheless, we will briefly discuss these issues in

Section 5. In summary, we limit ourselves to the kinematics in the form given by (6). Consequently, the space of objects, now called the space of kinematics, takes the form $V = C^\infty(R^n, R^m)$. Obviously we endow V with the inner product $\langle \cdot, \cdot \rangle_V$ being a usual L^2 inner product, i.e.,

$$\langle k_1, k_2 \rangle_V = \int_{R^n} k_1^\top(x) k_2(x) \, \mathrm{d}x, \quad k_i \in V. \tag{7}$$

It is easy to check that V is a vector space.

To model the transformations, we recall that in calibration by diffeomorphisms, two diffeomorphisms are considered: φ and ψ, one acting on the left (ψ) and the other on the right (φ) such that the action on an element k becomes $\psi \circ k \circ \varphi^{-1}$.

We define the group of transformations as a Lie group G, specifically as the Cartesian product of two Lie groups F and H, $G = F \times H$. Thus, any element $g = (f, h) \in G$ has two components, where $f \in F$ and $h \in H$. The neutral element $e \in G$ consists of the neutral elements $e_F \in F$ and $e_H \in H$. The group operation is component–wise and is inherited from F and H: $g_1 \cdot g_2 = (f_1 \cdot f_2, h_1 \cdot h_2)$, $g_1, g_2 \in G$. The Cartesian product of Lie groups is itself a Lie group, thus all axioms and properties hold. Specifically, the group G will act on the element k of V by $g \cdot k = h \circ k \circ f^{-1}$. It is easy to check that the action is a left action.

In the previous section, we introduced the notion of a Lie algebra to specify ordinary differential equations (ODEs) on the Lie group. The Lie algebra of a Lie group is the tangent space in the identity element. In our case, the Lie algebra $\mathfrak{g} = T_e G$ is the direct sum of the Lie algebras of F and H, i.e., $\mathfrak{g} = \mathfrak{f} \oplus \mathfrak{h}$. This allows us to specify the ODEs. For $g_\vartheta = (\varphi_\vartheta, \psi_\vartheta) \in G$ and $u_\vartheta = (v_\vartheta, w_\vartheta) \in \mathfrak{g}$, the system of ODEs becomes

$$\begin{cases} \frac{\partial \varphi_\vartheta}{\partial \vartheta} = v_\vartheta \cdot \varphi_\vartheta, & \varphi_0 = e_F, \\ \frac{\partial \psi_\vartheta}{\partial \vartheta} = w_\vartheta \cdot \psi_\vartheta, & \psi_0 = e_H. \end{cases} \tag{8}$$

The last piece of notation to quantify the deformations is the inner product $\langle \cdot, \cdot \rangle_\mathfrak{g}$, which, for the introduced Lie group G, splits into the sum of the inner products of the corresponding Lie algebras

$$\langle \cdot, \cdot \rangle_\mathfrak{g} = \langle \cdot, \cdot \rangle_\mathfrak{f} + \langle \cdot, \cdot \rangle_\mathfrak{h}. \tag{9}$$

3.2. Calibration by diffeomorphisms. Leveraging the introduced framework, we can formally address the main problem of robot calibration. We establish the space of objects on which we act by a group of diffeomorphisms as the space $C^\infty(X, Y)$ of smooth mappings between the internal space X and the external space Y. Given that we are calibrating the kinematics of a robot, it is clear that V consists of kinematic mappings. Hence, we define V as the space of kinematics.

As we already mentioned, we constrain ourselves to robot kinematics that can be expressed in coordinates, with $X = \mathbb{R}^n$ and $Y = \mathbb{R}^m$, so $V = C^\infty(\mathbb{R}^n, \mathbb{R}^m)$.

To maintain consistency with calibration by diffeomorphisms, we define the group of transformations as $G = \mathrm{Diff}(X) \times \mathrm{Diff}(Y) = \mathrm{Diff}(\mathbb{R}^n) \times \mathrm{Diff}(\mathbb{R}^m)$. Due to numerical and computational constraints, it is not practical to work with the entire group of diffeomorphisms G. Instead, we focus on a more manageable subgroup generated by the flow of appropriate ordinary differential equations (ODEs). This approach is rooted in considering a group of diffeomorphisms arising from an admissible space of vector fields, as thoroughly detailed in the work of Younes (2019).

The process begins by selecting a space of vector fields $\mathcal{V}$ that is admissible, meaning it is continuously embedded in $C_0^1(\mathbb{R}^d, \mathbb{R}^d)$. An admissible space of vector fields ensures that the vector fields and their first derivatives vanish at infinity, providing the necessary regularity and decay properties. The group of diffeomorphisms, $\mathrm{Diff}_\mathcal{V}$, is then defined as the set of diffeomorphisms that are flows from time 0 to 1 of the vector fields in $\mathcal{V}$. This means that any diffeomorphism in $\mathrm{Diff}_\mathcal{V}$ can be represented as the result of integrating a vector field from the chosen space $\mathcal{V}$ over a unit time interval. Consequently, the elements of $\mathrm{Diff}_\mathcal{V}$ inherit the smoothness properties of $\mathcal{V}$, ensuring the transformations are sufficiently smooth for practical purposes.

For our specific application, we choose the space H^∞, which is the intersection of all Sobolev spaces. The Sobolev spaces H^k are function spaces that provide a measure of smoothness by considering both the function and its derivatives up to a certain order. The intersection H^∞ includes functions that are infinitely differentiable and have all their derivatives in L^2, ensuring a high degree of smoothness. By selecting H^∞, we ensure that the vector fields used to generate our diffeomorphisms are as smooth as possible, which is coherent with the original setting of calibration by diffeomorphisms.

Thus, we define G as $\mathrm{Diff}_\mathcal{V}(X) \times \mathrm{Diff}_\mathcal{W}(Y)$, consisting of diffeomorphisms that emerge as the flow of vector fields in the product space $\mathcal{V} \times \mathcal{W} = H^\infty(X) \times H^\infty(Y)$, i.e.,

$$\begin{cases} \frac{\partial \varphi_\vartheta}{\partial \vartheta} = v_\vartheta(\varphi_\vartheta), & \varphi_0 = \mathrm{id}_X, \\ \frac{\partial \psi_\vartheta}{\partial \vartheta} = w_\vartheta(\psi_\vartheta), & \psi_0 = \mathrm{id}_Y, \end{cases} \tag{10}$$

for $g_\vartheta = (\varphi_\vartheta, \psi_\vartheta) \in G$ and $u_\vartheta = (v_\vartheta, w_\vartheta) \in \mathcal{V} \times \mathcal{W}$.

To make the introduction complete we shall choose the inner products and dual pairings for $\mathfrak{g}$ and V. For the former one inner product takes the form

$$\langle u_1, u_2 \rangle_\mathfrak{g} = \langle v_1, v_2 \rangle_\mathcal{V} + \langle w_1, w_2 \rangle_\mathcal{W}, \quad u_i = (v_i, w_i) \in \mathfrak{g}, \tag{11}$$

where the inner products on the right hand side are the inner products for the appropriate admissible vector space,

i.e.,

$$\langle v_1, v_2\rangle_{\mathcal{V}} = \int_{R^n} v_1^\top(x) L_{\mathcal{V}} v_2(x)\,\mathrm{d}x, \quad v_1, v_2 \in \mathcal{V},$$

with $L_{\mathcal{V}}$ being a positive definite, self-adjoint, differential operator. Analogous definition holds for $\langle\cdot,\cdot\rangle_{\mathcal{W}}$. One should notice that to be compatible with the H^∞ space the chosen operator shall be of infinite order, i.e., it is a power series of differentials. In similar fashion we introduce the dual pairing between $\mathfrak{g}$ and $\mathfrak{g}^* = \{(L_{\mathcal{V}}v, L_{\mathcal{W}}w),\ (v,w) \in \mathfrak{g}\}$, i.e., for $u = (v,w) \in \mathfrak{g}$, $\upsilon = (\alpha,\beta) \in \mathfrak{g}^*$, we get

$$\langle v, u\rangle_{\mathfrak{g}^*\times\mathfrak{g}} = \langle \alpha, v\rangle_{\mathcal{V}^*\times\mathcal{V}} + \langle \beta, w\rangle_{\mathcal{W}^*\times\mathcal{W}}, \tag{12}$$

so the $\flat$ map for the inner product $\langle\cdot,\cdot\rangle_{\mathfrak{g}}$ is given by $u^\flat_\vartheta = (v,w)^\flat_\vartheta = (L_{\mathcal{V}}v, L_{\mathcal{W}}w)$. For the case of the space of kinematics we choose L^2 inner product and canonical pairing thus

$$\langle k_1, k_2\rangle_V = \int_{R^n} k_1^\top(x) k_2(x)\,\mathrm{d}x, \quad k_i \in V, \tag{13}$$

and

$$\langle \pi, k\rangle_{V^*\times V} = \int_{R^n} \pi^\top(x) k(x)\,\mathrm{d}x, \quad k \in V, \pi \in V^*, \tag{14}$$

then the $\flat$ map is the identity mapping $k^\flat_\vartheta = k$.

As we already mentioned the problem may be reformulated analogously to the optimization problem with the cost function (4). Considering our case, we shall compute appropriate mappings (5). Let us start with computing the fundamental vector field associated with the action of the group $G - \zeta_u$. This can be done as follows, for a given $u = (v,w) \in \mathfrak{g}$ and $k \in V$ with g_ϑ being a curve such that $g_0 = (Id_X, Id_Y)$ and $\left.\frac{\partial g_\vartheta}{\partial\vartheta}\right|_{\vartheta=0} = u$,

$$\begin{aligned}\zeta_u(k) &= \left.\frac{\partial}{\partial\vartheta}\right|_{\vartheta=0} g_\vartheta \cdot k \\ &= \left.\frac{\partial \psi_\vartheta(k(\varphi_\vartheta^{-1}))}{\partial\vartheta}\right|_{\vartheta=0} \\ &\quad + D\left(\psi_\vartheta\left(k(\varphi_\vartheta^{-1})\right)\right)\Big|_{\vartheta=0} \cdot \left.\frac{\partial\varphi_\vartheta^{-1}}{\partial\vartheta}\right|_{\vartheta=0} \\ &= w(k) - Dk\cdot v. \end{aligned} \tag{15}$$

Having defined ζ_u mapping, the momentum map can be computed in the following way:

$$\begin{aligned}&\langle k\diamond\pi, u\rangle_{\mathfrak{g}^*\times\mathfrak{g}} = \langle \pi, \zeta_u(k)\rangle_{V^*\times V} \\ &= \int_{R^n} \pi^\top(x) w(k(x))\,\mathrm{d}x - \int_{R^n} \pi^\top(x) Dk(x)\cdot v(x)\,\mathrm{d}x \\ &= \langle(-Dk^\top\pi, \pi), (v,w)\rangle_{\mathfrak{g}^*\times\mathfrak{g}}. \end{aligned} \tag{16}$$

To compute the map $T_k^*\zeta_u$ we shall consider the tangent lifted action and takes its dual. Thus,

$$\begin{aligned}T_k\zeta_u(U) &= \left.\frac{\partial}{\partial\vartheta}\right|_{\vartheta=0} \zeta_u(k_\vartheta) \\ &= \left.\frac{\partial}{\partial\vartheta}\right|_{\vartheta=0} (w(k_\vartheta) - Dk_\vartheta\cdot v) \\ &= Dw(k)U - DU\cdot v, \end{aligned} \tag{17}$$

where $u \in \mathfrak{g}$, k_ϑ is a curve in V with $k_0 = k$ and $\left.\frac{\partial k_\vartheta}{\partial\vartheta}\right|_{\vartheta=0} = U$. Considering the dual pairing

$$\langle T_k^*\zeta_u(P), U\rangle_{V^*\times V} = \langle P, T_k\zeta_u(U)\rangle_{V^*\times V} \tag{18}$$

which according to (14) and using the integration by parts may be rewritten as

$$\begin{aligned}&\int_{R^n} P^\top(x)\left(Dw(k(x))U(x) - DU(x)\cdot v\right)\mathrm{d}x \\ &= \int_{R^n} P^\top(x) Dw(k(x))U(x)\,\mathrm{d}x \\ &\quad + \int_{R^n} \mathrm{div}(P(x)v^\top(x))U(x)\,\mathrm{d}x \\ &= \langle (Dw(k))^\top P + \mathrm{div}(Pv^\top), U\rangle_{V^*\times V}. \end{aligned} \tag{19}$$

Finally, we get

$$\begin{aligned}&\langle T_k^*\zeta_u(P), U\rangle_{V^*\times V} \\ &\quad = \langle (Dw(k))^\top P + \mathrm{div}(Pv^\top), U\rangle_{V^*\times V}. \end{aligned} \tag{20}$$

Now, we may formulate our problem as follows. For given nominal kinematics k_0 and actual kinematics k ($k_0, k \in V$) find $P_0 \in V^*$ that minimizes

$$E(P_0) = \frac{1}{2}\left\|k_0 \diamond P_0\right\|^2_{\mathfrak{g}} + \frac{1}{2\sigma^2}\left\|k_1 - k\right\|^2_V, \tag{21}$$

where k_1 is defined as the solution of the system of equations

$$\begin{cases} \frac{\partial k_\vartheta}{\partial\vartheta} = w_\vartheta(k_\vartheta) - Dk_\vartheta\cdot v_\vartheta, \\ \frac{\partial P_\vartheta}{\partial\vartheta} = -(Dw_\vartheta(k_\vartheta))^\top P_\vartheta - \mathrm{div}(P_\vartheta v_\vartheta^\top), \\ L_{\mathcal{V}} v_\vartheta = Dk_\vartheta^\top P_\vartheta, \\ L_{\mathcal{W}} w_\vartheta = P_\vartheta. \end{cases} \tag{22}$$

It is important to note that the Jacobian of the current kinematics k_ϑ must be computed at every evaluation of the differential equations. Unfortunately, an analytical expression is not feasible. Instead, we compute the Jacobian along the evolution curve using the following equation

$$\frac{\partial Dk_\vartheta}{\partial\vartheta} = Dw(k_\vartheta)Dk_\vartheta - Dk_\vartheta Dv_\vartheta. \tag{23}$$

By supplementing the system of equations (22) with (23), we can determine the initial momenta P_0 using a numerical optimization procedure.

Solving the above optimization problem effectively addresses the calibration issue. Starting from the nominal kinematics and the optimal initial momenta, the nominal kinematics can be evolved to match the actual kinematics using the equations (22). However, for simplicity, we assumed that the actual kinematics is already known. In practice, the actual kinematics is not directly available, and the objective is to reconstruct this model using sparse data obtained from measurements of joint positions and corresponding end-effector poses.

In the next section, we will demonstrate the application of the introduced formalism to scenarios where the actual kinematics is only accessible through sparse measurement data. This will address the challenge of reconstructing the actual kinematics model with limited information.

3.3. Implementation. As discussed in the previous section, the actual kinematics is not directly available to us as a functional mapping. Instead, we can sample the kinematics through measurements at discrete points in the internal and external spaces. This limitation necessitates adopting a more flexible approach that accommodates these constraints. With this understanding, we begin by formalizing the notion of measurements.

The robot's nominal kinematics, k_0, is represented as a mapping (6), typically obtained using a standard method such as the Denavit–Hartenberg algorithm. Let k denote the actual kinematics of the robot—the mapping we aim to determine. We assume that $k \in V$ and that it is accessible only through discrete measurements.

From a practical perspective, these measurements consist of N pairs of joint positions and their corresponding end-effector positions. The joint positions are denoted by $(x_1, \ldots, x_N)$, where $x_i \in \mathbb{R}^n$, and the corresponding end-effector positions are $\big(k(x_1), \ldots, k(x_N)\big) = (y_1, \ldots, y_N)$, with $y_i \in \mathbb{R}^m$.

This representation acknowledges that our understanding of k is derived from a finite set of discrete data points rather than a continuous mapping. Consequently, we must develop methods to effectively infer the overall kinematic behaviour of the robot from these sparse measurements.

Given these collections of measurements x and y, our objective is to find diffeomorphisms ψ and φ that transform the nominal kinematics k_0 to resemble the actual kinematics k. This can be expressed as

$$\psi \circ k_0 \circ \varphi^{-1} = k. \tag{24}$$

However, obtaining such transformations for the entire domain is often infeasible. Instead, we relax the problem by enforcing the transformation to match the kinematics at the measured points and interpolate between these points to approximate the kinematics over the domain.

To achieve this, we leverage the reproducing property of reproducing kernels to parametrize vector fields, overcoming previous technical challenges. This widely adopted method embeds the problem in a reproducing kernel Hilbert space (RKHS) (Younes, 2019), effectively reducing it from an infinite-dimensional problem to a finite-dimensional one based on the number of measurements.

A key outcome of the theory of RKHS is that every properly defined kernel K uniquely defines a corresponding RKHS (see, e.g., Saitoh and Sawano, 2016). By selecting a suitable kernel, we can construct an RKHS that imposes specific smoothness properties on vector fields. This correspondence can also be derived directly from bijective, self-adjoint differential operators (Younes, 2019). Specifically, for a given differential operator L, the reproducing kernel K is its inverse, $K = L^{-1}$, and may also be interpreted as the Green's kernel associated with L.

The considered spaces of vector fields $\mathcal{V}$ and $\mathcal{W}$ are both Hilbert spaces equipped with Sobolev inner products defined by the differential operators $L_\mathcal{V}$ and $L_\mathcal{W}$, respectively. We assume that the vector fields $v_\vartheta \in \mathcal{V}$ and $w_\vartheta \in \mathcal{W}$ belong to the RKHS associated with $\mathcal{V}$ and $\mathcal{W}$, with the reproducing kernels $K_\mathcal{V}$ and $K_\mathcal{W}$ corresponding to $L_\mathcal{V}$ and $L_\mathcal{W}$.

What sets RKHS apart from general Hilbert spaces is its reproducing kernel, which enables the straightforward integration of smoothness and other functional properties into optimization processes. This characteristic is particularly valuable for calibrating robot kinematics from sparse data. In particular, it allows for interpolation of vector fields (10) at arbitrary locations, e.g., v_ϑ at particular point x may be computed with use of the reproducing property as follows

$$v_\vartheta(x) = \int_X K_\mathcal{V}(x, \xi)\alpha(\vartheta, \xi)\,\mathrm{d}\xi, \tag{25}$$

where $K_\mathcal{V}(x, \xi)$ represent the reproducing kernel for $\mathcal{V}$, while $\alpha(\vartheta, \xi)$ and $\beta(\vartheta, \eta)$ are vectors in $\mathbb{R}^m$ that serve as weighting coefficients in the kernel construction for multi-dimensional vector fields (as discussed in more detail by Younes (2019) and Carmeli *et al*. (2006)).

In practical scenarios involving a finite set of N sample points, the approximation of the vector fields may be evaluated with use of the following formulas:

$$\begin{aligned} v_\vartheta(x) &= \sum_{i=1}^{N} K_\mathcal{V}(x, \xi_i)\alpha_i(\vartheta), \\ w_\vartheta(y) &= \sum_{i=1}^{N} K_\mathcal{W}(y, \eta_i)\beta_i(\vartheta). \end{aligned} \tag{26}$$

Glueing the introduced pieces, the calibration by diffeomorphisms boils down to solving the following optimization problem. Given the nominal kinematics k_0 and the measurements $(x_i, y_i),\ i = 1, \ldots, N$, taken from the actual kinematics k, where $k_0, k \in V$, find $P_0 \in V^*$ that minimizes

$$\begin{aligned} E(P_0) &= \frac{1}{2}\sum_{i,j=1}^{N} {P_0^i}^{\top} Dk_0(x_i) K_{\mathcal{V}}(x_i, x_j) Dk_0^{\top}(x_j) P_0^j \\ &\quad + \frac{1}{2}\sum_{i,j=1}^{N} {P_0^i}^{\top} K_{\mathcal{W}}(k_0(x_i), k_0(x_j)) P_0^j \\ &\quad + \frac{1}{2\sigma^2}\sum_{i=1}^{N} \|k_1(x_i) - y_i\|_2^2 , \end{aligned} \tag{27}$$

with respect to

$$\begin{cases} \frac{\partial k_\vartheta(x_i)}{\partial \vartheta} = w_\vartheta(k_\vartheta(x_i)) - Dk_\vartheta(x_i)\cdot v_\vartheta(x_i), \\ \frac{\partial P_\vartheta^i}{\partial \vartheta} = -(Dw_\vartheta(k_\vartheta(x_i)))^{\top} P_\vartheta^i - \operatorname{div}(P_\vartheta^i v_\vartheta^{\top}(x_i)), \\ \frac{\partial Dk(x_i)}{\partial \vartheta} = Dw(k_\vartheta(x_i)) Dk_\vartheta(x_i) - Dk_\vartheta(x_i) Dv_\vartheta(x_i), \\ v_\vartheta(x_i) = \sum_j^N K_{\mathcal{V}}(x_i, x_j) Dk_\vartheta(x_j)^{\top} P_\vartheta^j, \\ w_\vartheta(y_i) = \sum_j^N K_{\mathcal{W}}(y_i, y_j) P_\vartheta^j, \end{cases} \tag{28}$$

where $k_1(x_i)$ is a solution of the ODEs above evaluated at the point $\vartheta = 1$.

The procedure driving one towards calibrated kinematics may be summarized in the following steps:

1. Design a nominal kinematics model using one of the common procedures, e.g., Denavit–Hartenberg, product of exponentials.

2. Take N measurements of the joint positions and corresponding end-effector poses.

3. Find the initial momenta P_0 for chosen reproducing kernels and algorithm parameters by solving (27).

4. Online evaluation. The calibrated kinematics is encoded in the initial momenta and the nominal kinematics, to obtain its value at the particular point ξ one have to solve for $\vartheta = 1$, the following system of ODEs

$$\begin{cases} \frac{\partial k_\vartheta(\xi)}{\partial \vartheta} = w_\vartheta(k_\vartheta(\xi)) - Dk_\vartheta(\xi)\cdot v_\vartheta(\xi), \\ \frac{\partial Dk(\xi)}{\partial \vartheta} = Dw(k_\vartheta(\xi)) Dk_\vartheta(\xi) - Dk_\vartheta(\xi) Dv_\vartheta(\xi), \\ v_\vartheta(x_i) = \sum_j^N K_{\mathcal{V}}(x_i, x_j) Dk_\vartheta(x_j)^{\top} P_\vartheta^j, \\ w_\vartheta(k_\vartheta(x_i)) = \sum_j^N K_{\mathcal{W}}(k_\vartheta(x_i), k_\vartheta(x_j)) P_\vartheta^j, \end{cases} \tag{29}$$

reusing P_ϑ^i and $k_\vartheta(x_i)$ the solution of the previous system of equations for the measurement points x_i.

3.4. Comparison with classical approach. In this section, we aim to provide a qualitative comparison between the classical approach and the one presented here. To highlight the differences, we will focus on the sets within which the solution is sought. As we observed, the space we operate in is the space of smooth mappings between X and Y, namely $\mathrm{C}^\infty(X, Y)$. Our objective is to find a mapping $k \in \mathrm{C}^\infty(X, Y)$ that describes the kinematics of the actual robot, which we do not know explicitly. Instead, we are equipped with a nominal model $k_n \in \mathrm{C}^\infty(X, Y)$ (a first-guess model constructed using prior knowledge of geometry and physical phenomena). The calibration procedure can thus be described as a method for improving our nominal model based on experimental data, such that the final outcome closely resembles the actual kinematics k. Broadly, this problem can be viewed as finding a path in $\mathrm{C}^\infty(X, Y)$ that connects k_n with k; see Fig. 2(a). The primary differences between the approaches can be uncovered by addressing the following questions: in which sets do we search for a solution, and how do we constrain these sets? In the classical approach, the set of attainable kinematics, $\mathcal{K}$, is described by the family of kinematics $K\colon X \times P \to Y$, parametrised by the model's parameter $p \in P$. In the case of a model obtained through the Denavit–Hartenberg algorithm, the parameters describe the geometry of the robot. Thus, the set can be formally expressed as

$$\mathcal{K} = \{K(\cdot, p) \mid \forall p \in P\} \subset \mathrm{C}^\infty(X, Y).$$

If a solution exists within the set above, i.e., if there exist parameters p_k describing the actual kinematics $k = K(\cdot, p_k)$, then the path $k_\vartheta = K(\cdot, p_\vartheta)$ between k_n and k may be induced by a path $p_\vartheta \in P$, such that $p_{\vartheta=0} = p_n$ and $p_{\vartheta=1} = p_k$; see Fig. 2(b). The main difficulty of this approach lies in selecting the family of kinematics, which requires a deep understanding of the phenomena involved in the robotic system to calibrate non-geometric discrepancies. In the case that the solution lies outside the set, one may find the parameters whose corresponding kinematics approximate the actual ones.

On the other hand, in the calibration of diffeomorphisms, the set of attainable kinematics is different. It consists of kinematics that are A-equivalent to the nominal one. This set can be formally described as the orbit of the nominal kinematics k_n

$$\mathcal{O}_{k_n} = \left\{\psi \circ k_n \circ \varphi^{-1} \mid (\varphi, \psi) \in \operatorname{Diff}(X) \times \operatorname{Diff}(Y)\right\},$$

where it is clear that $\mathcal{O}_{k_n} \subset \mathrm{C}^\infty(X, Y)$. In this case, if the actual kinematics k lies within the orbit, the path is given by $k_\vartheta = \psi_\vartheta \circ k_n \circ \varphi_\vartheta^{-1}$; see Fig. 2(c).

One may observe that the sets of attainable solutions are qualitatively different. In general, $\mathcal{O}_{k_n} \neq \mathcal{K}$, but there is a non-empty intersection between the sets. Of course, one may attempt to find a family of kinematics K such

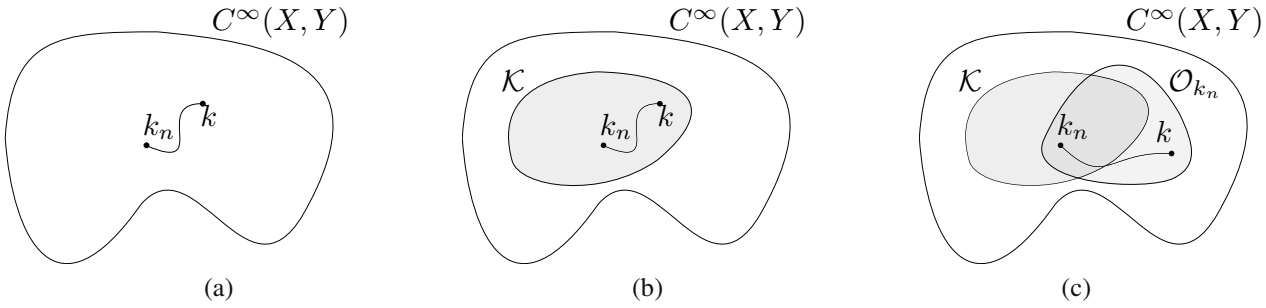

Fig. 2. Schematic figure visualizing the idea of manipulator calibration as a path search in $C^\infty(X,Y)$ and the sets of solutions: in general (a), model identification (b), calibration by diffeomorphisms (c).

that $\mathcal{O}_{k_n} \subset \mathcal{K}$, but in practice, this appears difficult. In such cases, the methodology introduced here allows one to find a solution outside the set $\mathcal{K}$ that is diffeomorphically equivalent to the nominal kinematics k_n. On the other hand, one may observe that there are kinematics attainable by the classical approach which cannot be attained through calibration by diffeomorphisms. These kinematics are not diffeomorphically equivalent to the nominal kinematics. It should be pointed out that, in the proposed practical implementation, the method is further constrained by the number of measurements and the considered kernels. However, even with these constraints, there is a noticeable increase in the accuracy of the calibrated kinematics, as demonstrated in the next section. One should view the proposed method as a complementary approach rather than a substitute. Future developments of the method should consider combining both approaches.

4. Numerical experiments

Based on the abstract formulation of the image registration problem, we introduced a novel computational framework utilizing the calibration by diffeomorphisms approach for robot manipulator kinematics calibration, originally presented by Tchoń (1992). Specifically, the k_1 solution to the system of differential equations (3) minimizes the optimization task's cost function (2), thereby redefining the robot kinematics calibration problem.

To evaluate the mathematical findings, we conducted three simulation experiments on the double pendulum, introducing the following types of discrepancies to the nominal kinematics: geometric discrepancies (such as variations in link length parameters), gravitational bending, and artificially induced large diffeomorphic discrepancies. The simulations followed the procedure described in Section 3.3. For implementation details, please refer to the work of Orozco and Ratajczak (2025).

The nominal kinematics of the double pendulum used as the test-bed in our experiment had the form

$$k(x) = \begin{pmatrix} l_1 \cos(x_1) + l_2 \cos(x_1 + x_2) \\ l_1 \sin(x_1) + l_2 \sin(x_1 + x_2) \end{pmatrix}, \qquad (30)$$

where $l_1 = 1$ and $l_2 = 0.5$. The kinematics of an actual robot used in those experiments as the ground truth was simulated as the nominal one perturbed by the appropriate discrepancies. As we already mentioned in the first scenario we perturbed the link length parameters, taking the values $l_1 = 0.98$ and $l_2 = 0.53$. In the second scenario, we model the gravitational based discrepancies relying on Book's model (Book, 1979). In the third one, the large diffeomorphic discrepancies had been obtained as $y = (k(x))^{-\frac{17}{19}} + t$, i.e., a nonlinear shearing followed by translation $t = \left(\begin{smallmatrix} 0.05 \\ -0.04 \end{smallmatrix}\right)$. For each scenario, from accordingly prepared kinematics, we generated a dataset of measurements, namely the pairs (x_i, y_{r_i}) for $i = 1, \ldots, 169$ taken from a regular grid of an actual robot joint positions x_i with the corresponding end-effector positions y_{r_i} to feed the calibration algorithm. The algorithm has been implemented with the use of Matlab framework exploiting built-in algebraic and differential equation solvers as well as the Kernel Operations (KeOps) library (Charlier *et al.*, 2021), supplying Matlab with functions for efficient calculations of kernel-related operations.

Figure 3 illustrates the evaluation of this calibration process for the kinematics of a double pendulum, taking into account both geometric and non-geometric discrepancies. The heatmaps in the figure present the resulting error between the real robot's position and the kinematics prediction before and after calibration. These errors were measured at 3000 pseudo-randomly generated positions throughout the workspace, ensuring a comprehensive evaluation across different regions.

The shades of the points in the heatmaps depict the exponent of the norm of the error, providing a clear visual representation of the error magnitude. One can observe

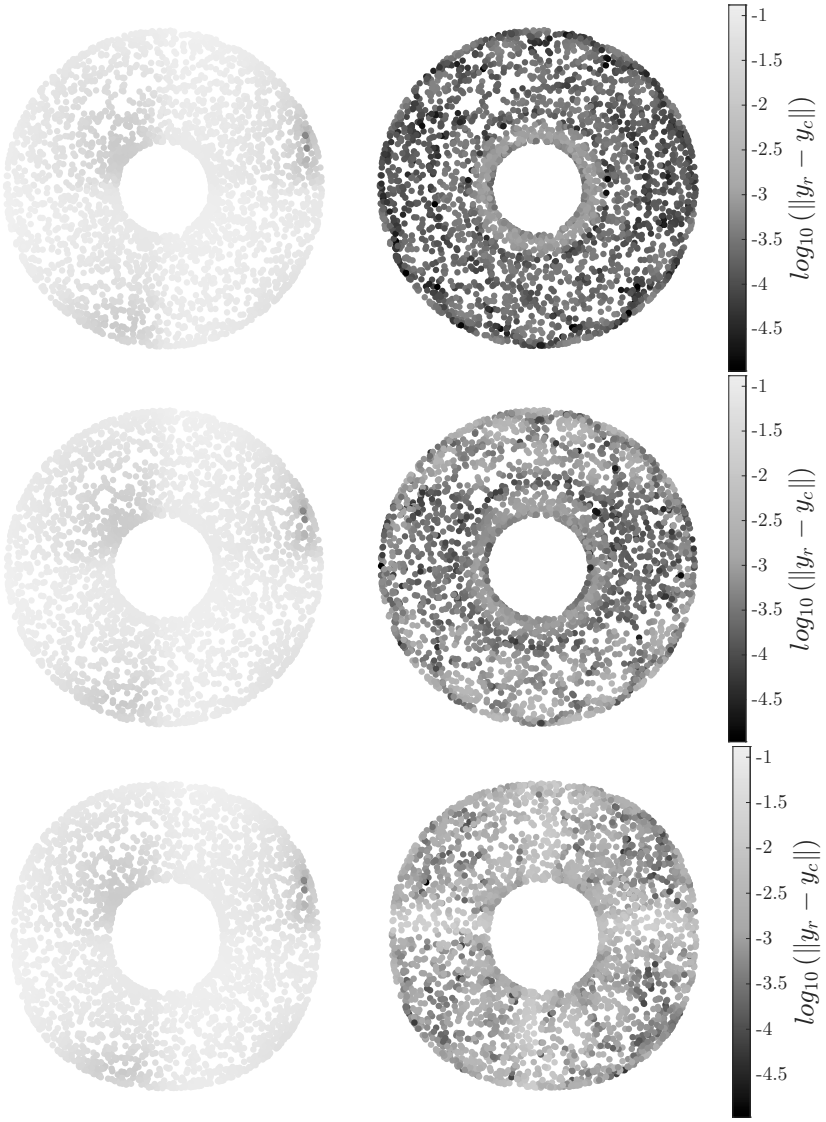

Fig. 3. Heatmaps present the resulting error between the position of the real robot and the kinematics model before (left column) and after calibration by diffeomorphisms (right column). The kinematics have been perturbed with the following discrepancies: discrepancies in link lengths (top), gravitational bending (middle), and large diffeomorphism (bottom).

that the calibration process significantly reduces the error, with a decrease of about one to three orders of magnitude, depending on the region of the workspace and the nature of the discrepancies. This substantial reduction in error highlights the effectiveness of the calibration process in improving the accuracy of the kinematic predictions, thereby enhancing the overall performance and reliability of the double pendulum system.

5. Discussion and future work

We demonstrated that the introduced method effectively handles kinematics expressed in coordinates. Despite its potential, it is crucial to extend this approach to a broader class of robot manipulator kinematics that map the configuration space to a subgroup of the Euclidean motion group. Several challenges arise in generalizing the method for such kinematics. The primary challenge is efficiently designing a smooth nonlinear vector field on the special Euclidean group $SE(3)$. While the machinery of reproducing kernel Hilbert space efficiently addresses this problem in Euclidean spaces, leveraging the method for $SE(3)$ requires constructing an appropriate RKHS on the $SE(3)$ manifold. De Vito *et al.* (2021) provides insights into this construction.

When setting the task space to a special Euclidean group, the space of objects is no longer a vector space, necessitating adjustments in methodology, including the evolution equations and the matching term in the cost

function. The landmark LDDMM approach on manifolds, as explored in the work of Glaunès *et al*. (2004), offers considerations.

The presented calibration method is highly general and applicable to models expressed as mappings between Euclidean spaces, making it a valuable tool in system identification. For example, it can be employed for the identification or calibration of nonlinear sensor characteristics or any other system that may be characterized by static models.

The large deformation diffeomorphic metric mapping framework, beyond producing optimal deformations for image registration, serves as a powerful tool for quantitative shape analysis in computational anatomy. Its formulation gives rise to the field of diffeomorphometry, a metric study of shapes and imagery, which opens new opportunities for analysing and inferring anatomical shapes in medical sciences. One promising application of using calibration by diffeomorphisms based on the LDDMM approach is leveraging diffeomorphometric features as theoretical foundations for predictive maintenance. This direction appears to be highly valuable and worth exploring further.

6. Summary

In this paper, we introduce the mathematical foundation for a novel computational method for calibration by diffeomorphisms, based on the LDDMM approach, which has not yet been applied within the field of robotics. This approach effectively addresses the calibration problem, as demonstrated both theoretically and through simulation experiments. Our methodology extends the concept of calibration by diffeomorphisms previously proposed by Tchoń (1992).

It is important to highlight that, unlike Tchoń's work, our method does not assume the nominal kinematics to be stable. Instead, the calibrating transformations are designed to be smooth and diffeomorphic, ensured by a regularization term in the cost function and the computation of final transformations as the flow of ordinary differential equations. Consequently, once the nominal kinematics are selected, we remain within the class of kinematics that are diffeomorphically equivalent to the nominal model.

However, this approach has its limitations, particularly in cases of unstable kinematics where minor parameter perturbations can significantly alter the topological structure of the mapping. For example, if the nominal kinematics are represented by a double pendulum with both links of equal length, transforming this nominal model into one with links of different lengths is impossible due to their lack of diffeomorphic equivalence. In such scenarios, only the best possible approximation can be achieved. To address this limitation, we propose relaxing the diffeomorphic constraints within the framework, enabling greater flexibility and facilitating more accurate transformations.

From practical and implementation perspectives, the method requires further investigation to evaluate its robustness against variations in the number, placement, and accuracy of measurements. Such an analysis could provide valuable insights into its practical applicability and identify potential limitations under real-world conditions. Those will be a key focus of our future work, as outlined in the discussion section.

References

Beg, M.F., Miller, M., Trouvé, A. and Younes, L. (2005). Computing large deformation metric mappings via geodesic flows of diffeomorphisms, *International Journal of Computer Vision* **61**(2): 139–157.

Bonilla, I., Mendoza, M., Campos-Delgado, D.U. and Hernández-Alfaro, D.E. (2018). Adaptive impedance control of robot manipulators with parametric uncertainty for constrained path-tracking, *International Journal of Applied Mathematics and Computer Science* **28**(2): 363–374, DOI: 10.2478/amcs-2018-0027.

Book, W.J. (1979). Analysis of massless elastic chains with servo controlled joints, *Journal of Dynamic Systems, Measurement, and Control* **101**(3): 187–192.

Bruveris, M. and Holm, D.D. (2015). *Geometry of Image Registration: The Diffeomorphism Group and Momentum Maps*, Springer, New York, pp. 19–56, DOI: 10.1007/978-1-4939-2441-7_2.

Carmeli, C., De Vito, E. and Toigo, A. (2006). Vector valued reproducing kernel Hilbert spaces of integrable functions and Mercer theorem, *Analysis and Applications* **04**(04): 377–408.

Charlier, B., Feydy, J., Glaunès, J.A., Collin, F.-D. and Durif, G. (2021). Kernel operations on the GPU, with autodiff, without memory overflows, *Journal of Machine Learning Research* **22**(74): 1–6.

De Vito, E., Mücke, N. and Rosasco, L. (2021). Reproducing kernel Hilbert spaces on manifolds: Sobolev and diffusion spaces, *Analysis and Applications* **19**(3): 363–396.

Gadringer, S., Gattringer, H., Müller, A. and Naderer, R. (2020). Robot calibration combining kinematic model and neural network for enhanced positioning and orientation accuracy, *IFAC-PapersOnLine* **53**(2): 8432–8437.

Glaunès, J.A., Vaillant, M. and Miller, M.I. (2004). Landmark matching via large deformation diffeomorphisms on the sphere, *Journal of Mathematical Imaging and Vision* **20**(1–2): 179–200.

Holm, D.D., Schmah, T., Stoica, C. and Ellis, D.C.P. (2009). *Geometric Mechanics and Symmetry: From Finite to Infinite Dimensions*, Oxford University Press, Oxford.

Nguyen, H.-N., Zhou, J. and Kang, H.-J. (2015). A calibration method for enhancing robot accuracy through integration of an extended Kalman filter algorithm and an artificial neural network, *Neurocomputing* **151**(3): 996–1005.

Orozco, R. and Ratajczak, A. (2025). Calibration by diffeomorphisms of robot manipulator kinematics: A novel approach, *Bulletin of the Polish Academy of Sciences Technical Sciences* **73**(2): 153230.

Pál, A., Vida, K., Mészáros, L. and Mező, G. (2015). Isotropic and anisotropic pointing models, *Experimental Astronomy* **41**(1–2): 1–15.

Saitoh, S. and Sawano, Y. (2016). *Theory of Reproducing Kernels and Applications*, Developments in Mathematics, 1st Edn, Springer, Singapore.

Scraggs, Ch., Smith, T., Sawyer, D. and Davis, M. (2021). Development of a non-parametric robot calibration method to improve drilling accuracy, *SAE International Journal of Advances and Current Practices in Mobility* **3**(3): 1152–1159, DOI: 10.4271/2021-01-0003.

Tchoń, K. (1992). Calibration of manipulator kinematics: A singularity theory approach, *IEEE Transactions on Robotics and Automation* **8**(5): 671–678.

Younes, L. (2019). *Shapes and Diffeomorphisms*, Applied Mathematical Sciences, Vol. 171, Springer, Berlin/Heidelberg.

Zhao, G., Zhang, P., Ma, G. and Xiao, W. (2019). System identification of the nonlinear residual errors of an industrial robot using massive measurements, *Robotics and Computer-Integrated Manufacturing* **59**: 104–114.

Zhong, X., Lewis, J. and N-Nagy, F.L. (1996). Inverse robot calibration using artificial neural networks, *Engineering Applications of Artificial Intelligence* **9**(1): 83–93.

Roberto Orozco earned his MSc in control engineering and robotics from Wrocław University of Science and Technology in 2020. Currently, he is a PhD student conducting research in robotics, with the focus on applying mathematical methods to system modelling and motion planning algorithms.

Joanna Ratajczak hold a DSc in the automation, electronics, electricals engineering and space technologies (2022) as well as a PhD in control engineering and robotics (2012) from the Wrocław University of Science and Technology. Her research interests include the application of mathematical methods in robotics, including system modelling and motion planning algorithms. She is currently an associate professor at the Faculty of Electronics, Photonics and Microsystems, Wrocław University of Science and Technology.

Received: 24 July 2024
Revised: 7 January 2025
Re-revised: 21 January 2025
Accepted: 25 February 2025